



Article

The Impact of PP-g-MAH on Mechanical Properties of Injection Molding of Long Glass Fiber/Polypropylene Pellets from Thermoplastic Pultrusion Process

Ponlapath Tipboonsri and Anin Memon *

Department of Industrial Engineering, Faculty of Engineering, Rajamangala University of Technology Thanyaburi (RMUTT), Klong Luang 12110, Thailand; ponlapath_t@mail.rmutt.ac.th

* Correspondence: anin.m@en.rmutt.ac.th

Abstract: Long fiber thermoplastic pellets are pellets containing discontinuous reinforced fibers and a matrix, offering excellent mechanical properties, good processability, recyclability, and low cost. Typically, commercial LFTP is manufactured through the hot melt impregnation process, combining extrusion and pultrusion. Although there is a thermoplastic pultrusion process for LFTP production, characterized by a simple machine and an easy method, its mechanical properties have not yet approached those of commercial LFTP. In improving the mechanical characteristics of LFTP manufactured via thermoplastic pultrusion, this research employed polypropylene-graft-maleic anhydride as a coupling agent during the injection molding procedure. The LFTP is composed of polypropylene material reinforced with glass fiber. Mechanical and physical properties of the LFTP were investigated by introducing PP-g-MAH at concentrations of 4, 8, and 12 wt% through injection molding. The results revealed that, at a 4 wt% concentration of PP-g-MAH, the LFTP composites exhibited heightened tensile, flexural and impact strengths. However, these properties began to decrease upon exceeding 4 wt% PP-g-MAH. The enhanced interfacial adhesion among glass fibers, induced by PP-g-MAH, contributed to this improvement. Nonetheless, excessive amounts of PP-g-MAH led to a reduction in molecular weight, subsequently diminishing the impact strength, tensile modulus, and flexural modulus. In LFTP composites, both tensile and flexural strengths exhibited a positive correlation with the PP-g-MAH concentration, attributed to improved interfacial adhesion between glass fibers and polypropylene, coupled with a reduction in fiber pull-out. Based on morphological analysis by SEM, the incorporation of PP-g-MAH improved interfacial bonding and decreased fiber pull-out. The presence of maleic anhydride in the LFTPc was confirmed through the utilization of FTIR spectroscopy. Mechanical properties of LFTP containing 4 wt% PP-g-MAH were found to be equivalent to or superior to those of commercial LFTP, according to the results of a comparative analysis.



Citation: Tipboonsri, P.; Memon, A. The Impact of PP-g-MAH on Mechanical Properties of Injection Molding of Long Glass Fiber/Polypropylene Pellets from Thermoplastic Pultrusion Process. *J. Manuf. Mater. Process.* **2024**, *8*, 53. <https://doi.org/10.3390/jmmp8020053>

Academic Editors: Patricia Krawczak and Ludwig Cardon

Received: 29 January 2024

Revised: 22 February 2024

Accepted: 23 February 2024

Published: 2 March 2024

Keywords: LFTP composite; thermoplastic pultrusion; long glass fiber reinforced polypropylene; PP-g-MAH



Copyright: © 2024 by the authors. Licensee MDPI, Basel, Switzerland. This article is an open access article distributed under the terms and conditions of the Creative Commons Attribution (CC BY) license (<https://creativecommons.org/licenses/by/4.0/>).

1. Introduction

Long fiber thermoplastic pellets (LFTPs) are plastic pellets composed of reinforced fibers and thermoplastic. The fibers embedded in the pellets are discontinuous and possess a length-to-diameter aspect ratio exceeding the critical aspect ratio [1–3]. Normally, LFTPs are utilized in compression and injection molding processes. Various industries, including automobile, sports, wind energy, military, aerospace, and electronics [4–6], employ LFTPs in manufacturing due to their superior mechanical properties, weight savings, improved damping, good processability, recyclability, corrosion resistance, and low cost [1,6,7]. Several types of thermoplastic matrices are used in the fabrication of LFTP, such as polyamide (PA), polymethyl methacrylate (PMMA), polyacrylonitrile–butadiene–styrene (ABS), and polypropylene (PP), among others [8–11]. These matrices are reinforced

with glass fiber and carbon fiber [12]. The popular type of LFTP incorporates glass fiber (GF) reinforcement in polypropylene (PP) due to its low density, low molding temperature, and cost-effectiveness [13–15]. Glass fiber provides high tensile stress and is also cost-effective [16,17]. The combination of glass fiber and polypropylene results in a composite with excellent mechanical properties, low density, and cost-effectiveness. The typical manufacturing process for LFTP involves a hot melt impregnation process, combining extrusion and pultrusion processes. Continuous reinforced fibers are drawn into the hot melt impregnation die, where molten thermoplastic from the extruder impregnates the reinforcing fibers. Subsequently, the material undergoes cooling and is subsequently cut into the desired length. LFTP products usually demonstrate dimensions of 6 to 25 mm in length and 2 to 4 mm in diameter [1,18,19].

Currently, achievements have been made in producing LFTP using the thermoplastic pultrusion process [20,21]. This method demonstrates comparable mechanical properties to the conventional process but incurs lower costs due to the absence of an extruder requirement in the machinery setup. Generally, pultrusion processes are used for the fabrication of constant cross-section and continuous composites. The advantages of this process include high mechanical properties of products, a high production rate, and low cost [22]. Pultrusion processes can fabricate both thermoplastic and thermoset composites [23]. Thermoplastics are gaining interest due to their recyclability, contributing to the reduction in environmental pollution problems [24]. Thermoplastic composites are highly ductile, tough to break, impact resistant, recyclable, and quickly processed [25,26]. Therefore, the thermoplastic pultrusion process is interesting to develop for adding new products, with the capability of fabricating LFTP through this method. In the process of manufacturing LFTP through thermoplastic pultrusion, continuous thermoplastic fibers and continuous fibers are drawn into the heated die. The thermoplastic fibers undergo melting at elevated temperatures, impregnating the fibers, followed by cooling and subsequent cutting into the required length [21,23]. Although LFTP is fabricated using thermoplastic pultrusion, which imparts good mechanical properties, its mechanical characteristics may not be sufficient when compared to some commercial LFTP products. Surface treatment is one among numerous techniques that can be implemented to boost the mechanical properties of composites. Interfacial adhesion is improved as a result of surface treatment of the fiber, which in turn leads to improvements in mechanical properties [27]. Using a coupling agent [28,29] is a popular method for surface treatment. GF and PP are treated with polypropylene-graft-maleic anhydride (PP-g-MAH), one such agent [30]. The incorporation of PP-g-MAH improves the mechanical properties of the GF/PP composite by enhancing interfacial adhesion [31,32].

The aim of this study is to improve the interfacial adhesion between GF and PP in the LFTP composite (LFTPc) by utilizing PP-g-MAH as a coupling agent. The preparation of LFTPc, which is made up of GF/PP, was carried out through the use of the injection molding process, alongside the incorporation of PP-g-MAH into this process. The LFTP was produced through the thermoplastic pultrusion process. The literature review indicates that PP-g-MAH has been widely used as a coupling agent to enhance interfacial adhesion, leading to a notable growth of mechanical properties by 10–40% [27,30,33–35]. In the literature review of PP composites reinforced with long glass fiber (LGF), GF is typically used at a volume fraction of 10–40 wt% in the composite [1,35,36], with most LFTPs in the literature being fabricated using the hot melt impregnation process. Therefore, this work differs in the manufacturing process of LFTP, which is fabricated using the thermoplastic pultrusion process: a method known for its cost-effectiveness and high productivity.

2. Materials and Methods

2.1. Materials

The thermoplastic pultrusion method was utilized to produce LFTP in this study. PP yarn with a density of 0.946 g/cm^3 (133 tex or 1200 denier) was purchased from Praditkorn Co., Ltd., Bangkok, Thailand, and GF yarn with a density of 2.620 g/cm^3 (EDR171200386) was purchased from China Jushi Co., Ltd., Tongxiang, China. The diameter and length of the LFTP are 3 mm and 10–12 mm, respectively. For injection, LFTP was combined with PP pellets (POLIMAXX 1100NK) that were purchased from Ircp Polyol Co., Ltd. in Bangkok, Thailand. As a coupling agent, PP-g-MAH was purchased from Merick Polymer Co., Ltd., Bangkok, Thailand.

2.2. Methods

The thermoplastic pultrusion technique was employed in this experiment for manufacturing LFTP, with the molding temperature ranging from 160 to 230 °C and the pulling speed set at 10 cm/min. In the process of manufacturing LFTP through thermoplastic pultrusion, continuous PP fibers and continuous glass fibers are drawn into the heated die. The PP fibers undergo melting at elevated temperatures, impregnating the glass fibers. This is followed by fan cooling and subsequent cutting into the required length using a plastic pellet cutting machine. The preheat die and heating die for the lab-scale thermoplastic pultrusion machine employed for manufacturing LFTP are both 645 mm in length. The cross-sectional length of both dies is 300 mm, while their taper length is 345 mm and their radius is 1 degree. A characteristic of the pultrusion die is its 3 mm diameter.

The LFTP consists of a combination of PP and GF with volume fractions of 87.03 and 12.97%, respectively. The determination of the volume fraction of LFTP employed the filling ratio equation outlined in the literature [20,21]. LFTP, characterized by a specified diameter of 3 mm and length ranging from 10 to 12 mm, as indicated in the literature [18] and aligned with commercial LFTP standards, was utilized. LFTP and virgin PP were mixed together in dry mixer, with a volume fraction of 15% by weight of GF. Subsequently, PP-g-MAH was added at weight concentrations of 4%, 8%, and 12% during the injection molding process. Intermediate materials were subjected to overnight drying at 100 °C in an oven before injection to eliminate moisture from PP-g-MAH, given that MAH is hygroscopic. The injection molding machine (LG model LGH-50N) was used to prepare LFTPc specimens for property testing. Molding temperature ranges were set between 170 and 190 °C, with an injection speed set at 100 mm/sec, injection pressure at 90 MPa, and holding pressure at 30 MPa. These parameters were adjusted according to the datasheet of virgin PP. Figure 1 displays the schematic of the experiment. Specimens were evaluated for their mechanical and physical properties.

2.3. Characterization and Measurement

2.3.1. Mechanical Properties

Mechanical testing, including impact, flexural, and tensile tests, was conducted to investigate the properties of LFTPc. A tensile test was performed in accordance with ASTM D638 [37] standards using a Hounsfield universal testing machine (Load 25 kN) at a testing speed of 50 mm/min. The dog bone type I structure was used for fabricating the tensile specimens. A flexural test was carried out, corresponding with the standards of ASTM D790 [38]. A Hounsfield universal testing machine was utilized, which consisted of a three-point bending model (load of 25 kN), a test speed of 1.30 mm/min, and a span length of 48 mm. The head speed was set according to ASTM D790 [38] standards. The impact properties of LFTPc were carried out using an impact Izod tester fitted with a 2J hammer in accordance with ASTM D256 [39] guidelines.

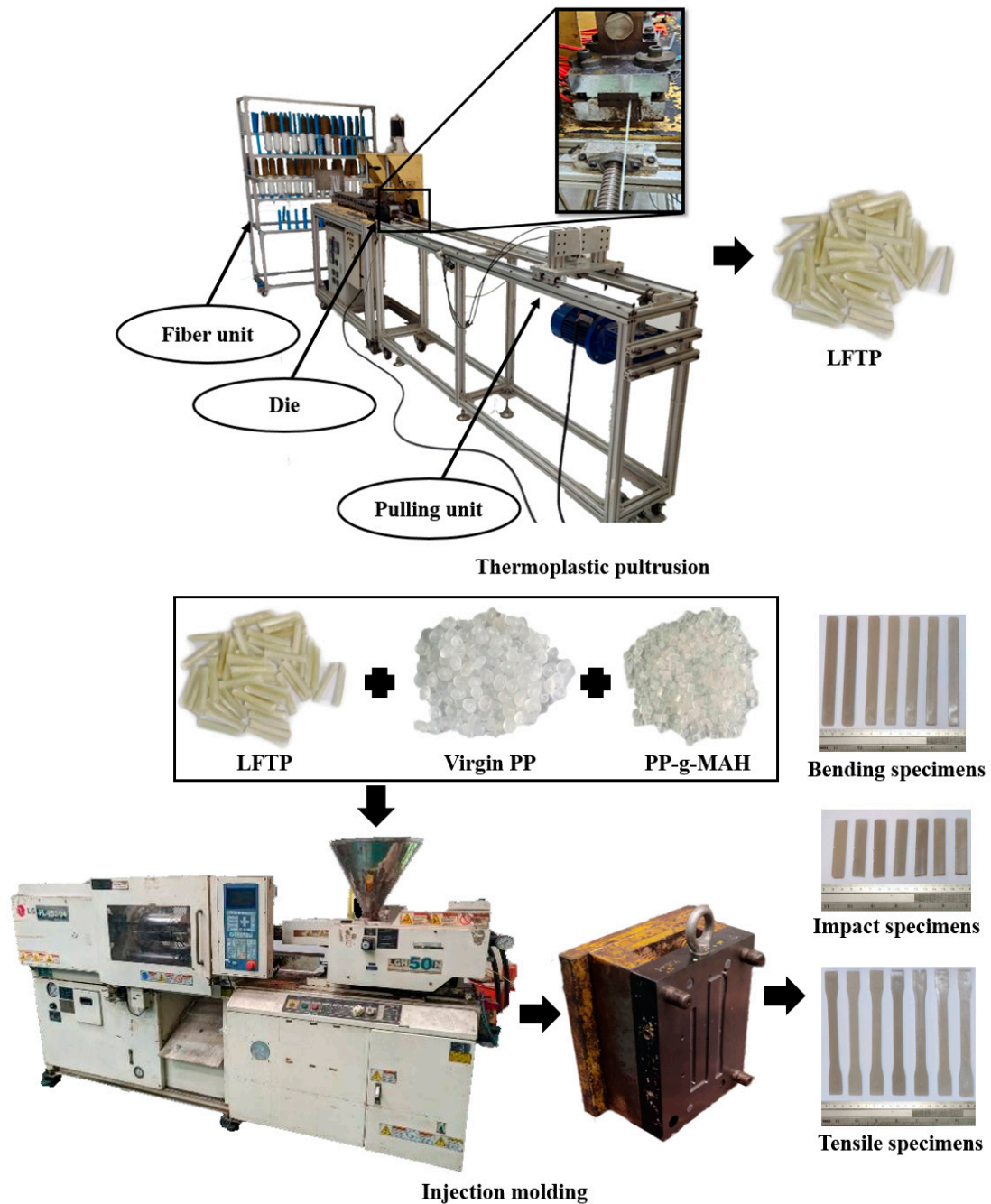


Figure 1. Preparing LFTP through the thermoplastic pultrusion process for injection molding.

2.3.2. Fiber Length Measurement

The fiber length of LFTPc was measured using specimens from injection molding. These specimens were placed on the black substrate of ceramic tiles and burned at a temperature of 500 °C for 2 h using a Nabertherm furnace. The decomposition of PP in LFTPc occurred due to the higher degradation temperature of PP, leaving only GF and ash. The GF was distributed, and the fiber length was measured using a microscope (Motic model SMZ-171) at 10× magnification. At least 1000 fibers were sampled and measured using the ImageJ program. The fiber count results were calculated by determining the number of fibers in each range of fiber length per total number of fibers. Figure 2 illustrates the fiber length measuring process of LFTPc.

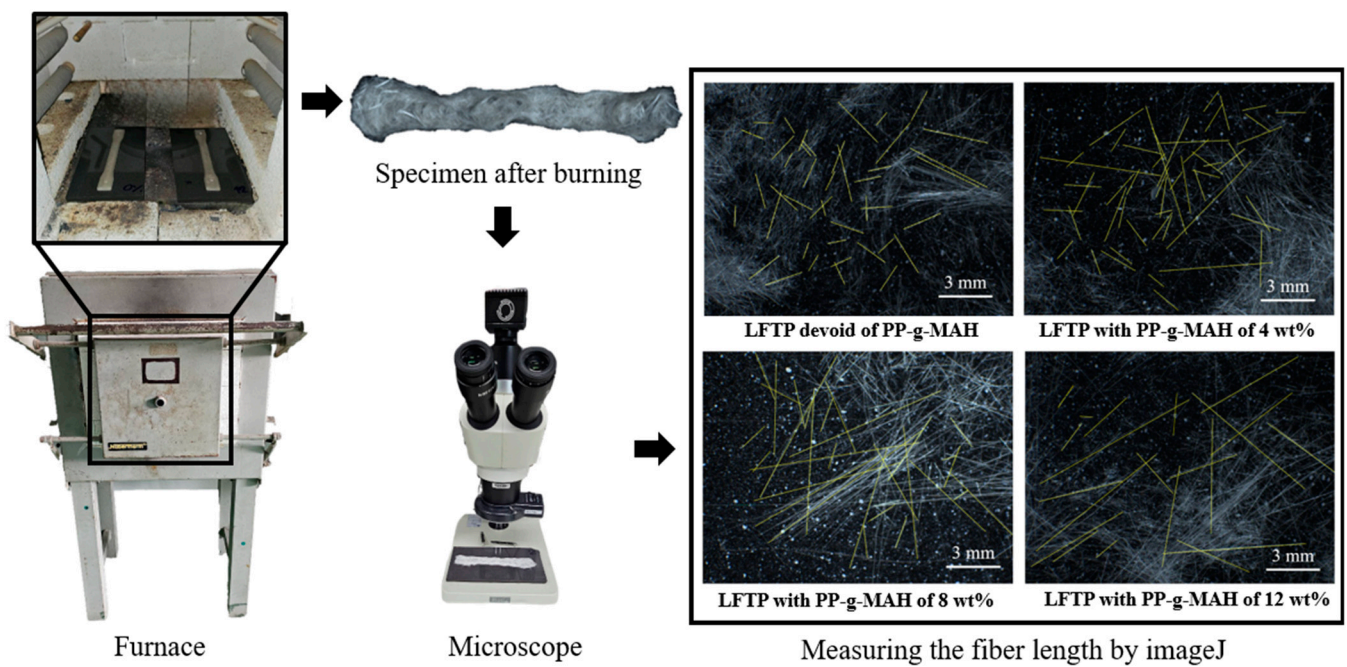


Figure 2. Fiber length measuring process of LFTPc.

2.3.3. FTIR Spectroscopy

The LFTPc specimens were examined for chemical composition using Fourier transform infrared spectroscopy (FTIR) measurement (using the Thermo Scientific Nicolet iS5, Waltham, MA, USA) to characterize their functional groups. The specimens were analyzed over a range of 4000 to 400 cm^{-1} .

2.3.4. Morphology

The surface morphology of LFTPc specimens was examined utilizing a scanning electron microscope (SEM), examining both the fiber pullout from the specimens and the interfacial adhesion between GF and PP (using the JEOL model JSM-5410LV, Tokyo, Japan). Specimens after the impact test were examined at $50\times$ and $500\times$ magnifications.

3. Results

3.1. The Influence of the Coupling Agent on the Mechanical Properties of the LFTPc

Both tensile modulus and tensile strength values are determined through tensile tests. The tensile modulus of LFTPc is illustrated in Figure 3 at varying concentrations of PP-g-MAH. Additionally, the characteristics of specimens during testing are depicted. It was found that the tensile modulus increased while the PP-g-MAH concentration was at 4 wt%, but it decreased when the PP-g-MAH concentration grew higher. For PP-g-MAH concentrations of 0, 4, 8, and 12 wt%, the tensile modulus values for the LFTPc were 2710, 3183, 2954, and 2830 MPa, respectively. The LFTPc, containing 4 wt% PP-g-MAH, exhibited a tensile modulus approximately 17.45% higher than that of the LFTPc devoid of PP-g-MAH, reaching its maximum tensile strength. Despite the decrease in tensile modulus beyond 4 wt% PP-g-MAH, these values remained greater than those of LFTP lacking PP-g-MAH.

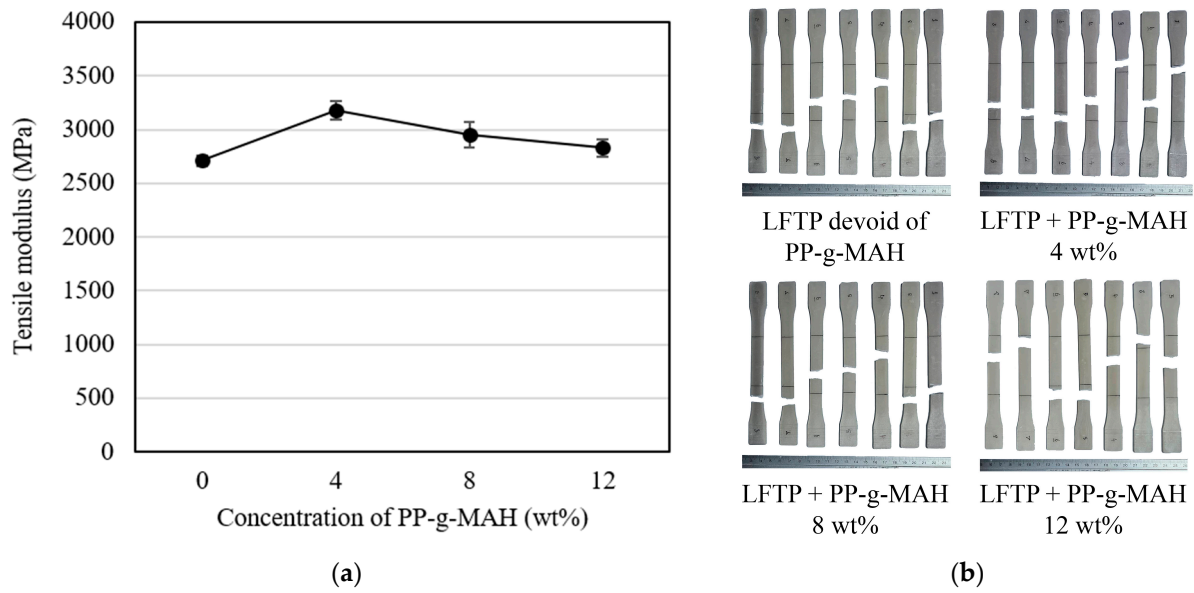


Figure 3. Correlation between (a) tensile modulus and the concentration of PP-g-MAH in LFTPc and (b) testing specimens.

Figure 4, which exhibits the results of employing various concentrations of PP-g-MAH, depicts the tensile strength of LFTPc. The results indicate that an increase in the amount of PP-g-MAH correlates with a related increase in the tensile strength. At PP-g-MAH concentrations of 0, 4, 8, and 12 wt%, the tensile strength values for the LFTPc were 38.92, 55.37, 59.84, and 61.98 MPa, respectively. The LFTPc with a 12 wt% PP-g-MAH component exhibited a tensile strength increase of approximately 59.24% compared to LFTPc devoid of PP-g-MAH.

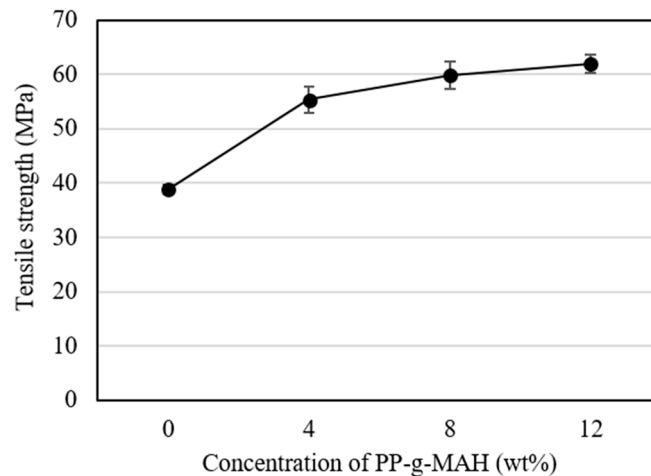


Figure 4. Correlation between tensile strength and the concentration of PP-g-MAH in LFTPc.

The results of testing specimens and the flexural modulus of the LFTPc with varying concentrations of PP-g-MAH are shown in Figure 5. Similar to the tensile modulus, the results indicate that the flexural modulus increased at a PP-g-MAH concentration of 4 wt% and reduced when the concentrations of PP-g-MAH surpassed 4 wt%. The flexural modulus values of LFTPc, with concentrations of PP-g-MAH at 0, 4, 8, and 12 wt%, were 1968, 2376, 2244, and 2146 MPa, respectively. The LFTPc containing a concentration of 4 wt% PP-g-MAH exhibited the greatest flexural modulus, showing an increase of approximately 20.73% compared to the LFTPc devoid of PP-g-MAH. In the same way that

the flexural modulus values exhibited a reduction when the concentrations of PP-g-MAH surpassed 4 wt%, they consistently remained at levels superior to those of the LFTPc devoid of PP-g-MAH.

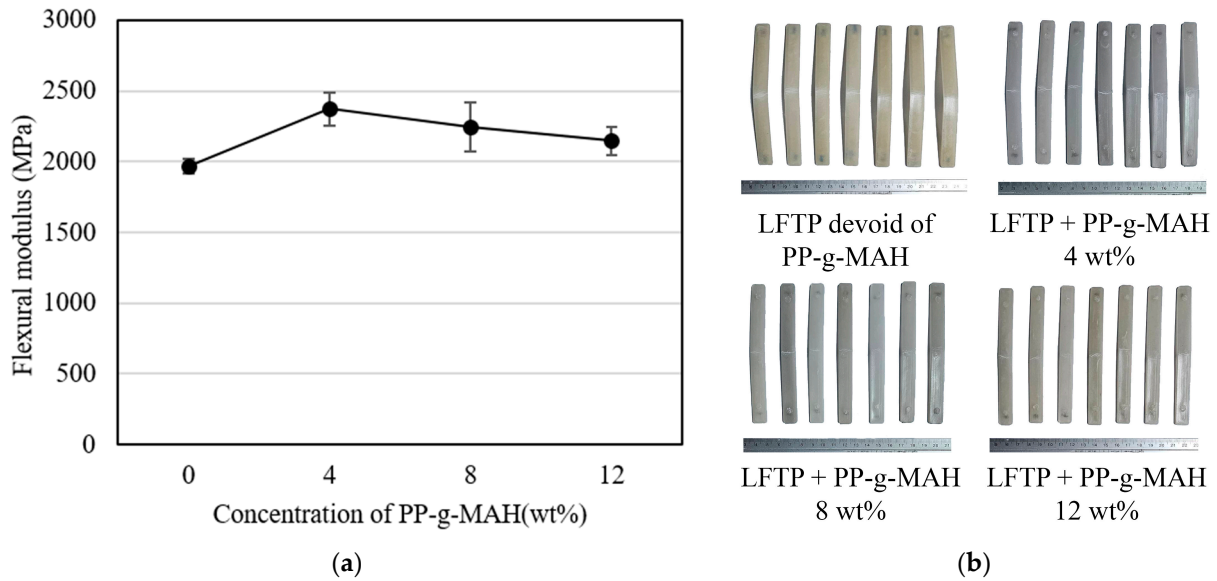


Figure 5. Correlation between (a) flexural modulus and the concentration of PP-g-MAH in LFTPc and (b) testing specimens.

Figure 6 presents an illustration of the flexural strength values of the LFTPc using various concentrations of PP-g-MAH. The results indicate that the flexural strength exhibited an increase in correlation with the concentration of PP-g-MAH. The respective flexural strengths of the LFTPc were obtained at 47.27, 68.16, 77.35 and 80.02 MPa, when the concentrations of PP-g-MAH were 0, 4, 8, and 12 wt%. The LFTPc containing 12 wt% PP-g-MAH demonstrated the maximum flexural strength values, an increase of approximately 69.66% in comparison to the LFTPc devoid of PP-g-MAH.

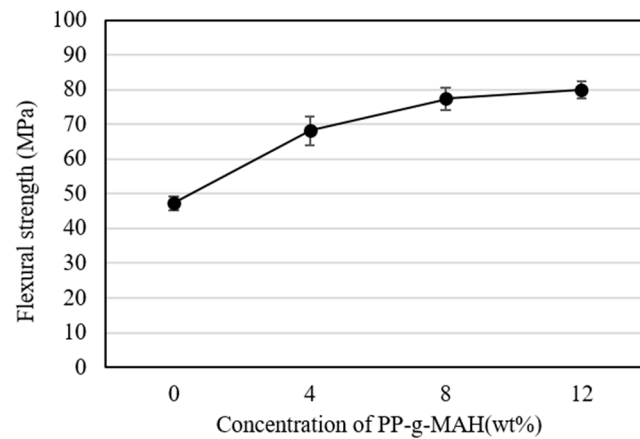


Figure 6. Correlation between flexural strength and the concentration of PP-g-MAH in LFTPc.

Figure 7 shows the impact strength of the LFTPc with varying concentrations of PP-g-MAH, along with features of the test specimens. Similar trends were observed in the impact strength data and the tensile and flexural modulus values. The impact strength increased at a concentration of 4 wt% PP-g-MAH and decreased beyond that point. The LFTPc exhibited impact strength values of 54.92, 82.57, 67.43, and 64.90 J/m, respectively, when PP-g-MAH was present in concentrations of 0, 4, 8, and 12 wt%. The LFTPc that incorporated 4 wt%

PP-g-MAH demonstrated the most significant increase in impact strength, approximately 50.34%, in comparison to the LFTPc that did not contain PP-g-MAH. While the impact property decreased with the concentration of PP-g-MAH surpassing 4 wt%, it continued to surpass that of the LFTPc devoid of PP-g-MAH. These differences corresponded with the tensile and flexural modulus values.

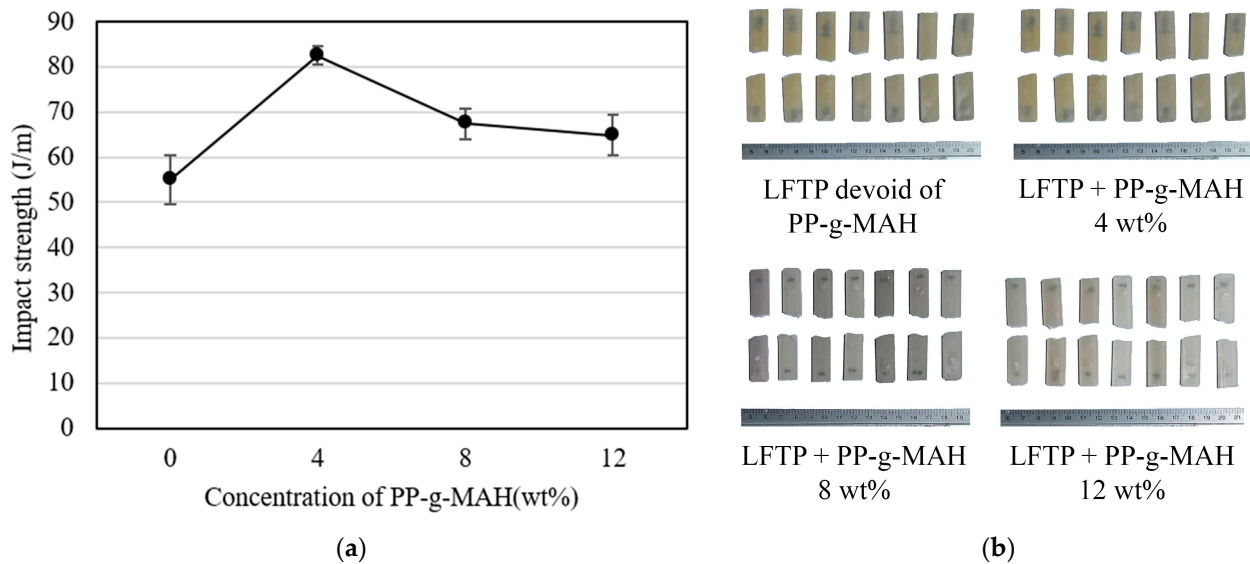


Figure 7. Correlation between (a) impact strength and the concentration of PP-g-MAH in LFTPc and (b) testing specimens.

The mechanical properties of the LFTPc were enhanced by the improved contact adhesion between PP and GF, which was caused by the incorporation of PP-g-MAH. Lin et al. and Fu et al. [27,36] elucidated the interaction between the hydroxyl groups of GF and the maleic anhydride of PP-g-MAH. The results align with the literature review [27,35,36,40], confirming the increased tensile modulus of the LFTPc when incorporated with PP-g-MAH.

The tensile modulus, flexural modulus, and impact strength values of the LFTPc, however, decreased at concentrations of PP-g-MAH beyond 4 wt% because, as explained by Lin et al. [27], PP-g-MAH can only enhance the interfacial adhesion between GF and PP; it cannot increase deformation resistance. Furthermore, a rise in the PP-g-MAH concentration results in a reduction in molecular weight [28]. The decrease in molecular weight affected the tensile strength and flexural strength, causing them to remain constant or decrease. In accordance with the literature, the elongation at break exhibited a rise as the molecular weight decreased [41]. Thus, when the amount of PP-g-MAH exceeded 4 wt%, the tensile and flexural modulus values decreased. Gumus [34] described the negative effects of PP-g-MAH on notched impact properties when the LFTPc incorporated a concentration of PP-g-MAH exceeding 4 wt%, resulting in decreased impact properties. In addition, the impact strength has a result in accordance with another study in the literature [36].

3.2. Fiber Length of LFTPc

The fiber length of GF decreased during the injection molding process due to the screw, cylinder, nozzle, and runner [35]. Figure 8 shows the residual fiber length of LFTPc with varying concentrations of PP-g-MAH. The results indicate that the fiber length of GF is distributed across the entire range, from 0.1 to 12 mm. The fiber length ranging from 0 to 2 mm exhibited the highest values, while the range of fiber length from 3 to 4 mm showed a decrease of only 5–15%. This finding suggests that LFTPc is reinforced by long fibers. Additionally, the percentage of fiber length in the range of 5 to 6 mm was 9–18%, providing clear evidence of reinforcement by long fibers. This is supported by the fact that short

fiber-reinforced composites typically have fiber lengths in the range of 0.1–0.5 mm. [18]. This evidence confirms the reinforcement by long fibers.

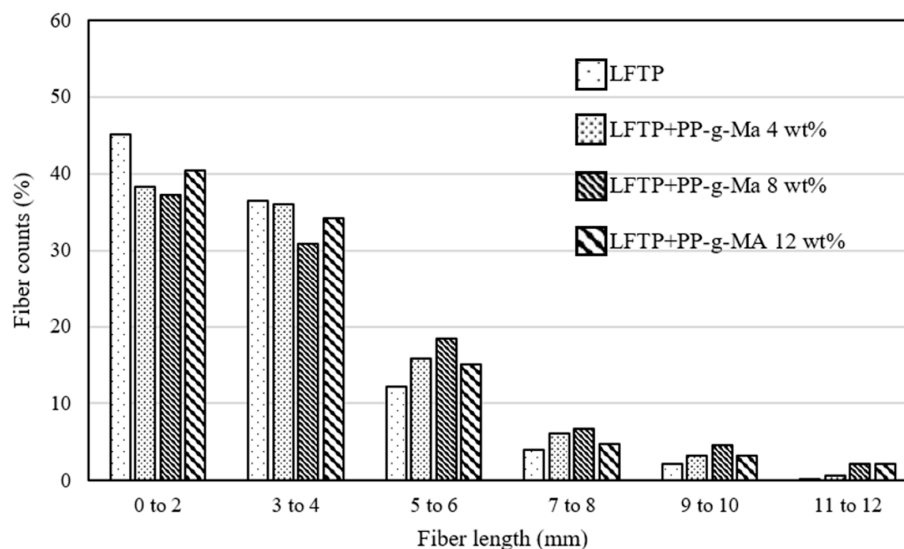


Figure 8. Residual fiber length of LFTP during the injection molding.

3.3. The Influence of the Coupling Agent on the Morphology of the LFTPc

Specimens were examined using SEM after the Izod impact test to investigate the surface morphology of the LFTPc with varying concentrations of PP-g-MAH, and the findings are shown in Figure 9. It was evident that the LFTPc's pull-out of GF and the spaces between them and PP was improved by the incorporation of PP-g-MAH. Figure 9b–e illustrates that the pull-out of fibers decreased as the concentration of PP-g-MAH increased. Consequently, the fiber pull-out and the interface between GF and PP were effectively improved by PP-g-MAH. Additionally, SEM images of the LFTPc containing varying concentrations of PP-g-MAH are displayed in Figure 10 at a 500× magnification. It was evident that as the amount of PP-g-MAH increased, the interstices between the GF and PP decreased. Furthermore, the incorporation of PP-g-MAH to the GF surface of the LFTPc resulted in an appearance of cohesive resin, which indicated a great interface between the GF and resin. Consequently, an improvement in the GF-PP interface and pull-out of fibers leads to an increase in mechanical characteristics. The images of the LFTPc with varying concentrations of PP-g-MAH corresponded with the literature review [27,36,40]. It effectively communicates that the mechanical properties of LFTPc were enhanced through the enhancement of interfacial adhesion between GF and PP, a result of the incorporation of PP-g-MAH.

3.4. FTIR Characterization

The spectra of virgin PP and the LFTPc with a varying PP-g-MAH content were examined at wave numbers ranging between 4000 and 400 cm^{-1} ; these spectra are displayed in Figure 11. The FTIR spectra exhibit consistent peaks at 2949 and 2915 cm^{-1} , corresponding to aliphatic C-H stretching, and at 1457 and 1375 cm^{-1} , indicating C-H bending, which, respectively, demonstrate the presence of PP in the LFTPc [34,42–44]. The carbonyl group (C=O) of the anhydride and the acid groups, respectively, is represented by peaks at 1740 and 1714 cm^{-1} in the FTIR spectra of the LFTPc with varying concentrations of PP-g-MAH [44–46]. It is confirmed that maleic anhydride is present in the LFTPc containing PP-g-MAH. Therefore, the presence of PP-g-MAH in LFTPc improved interfacial adhesion, as observed in SEM micrographs. This effect was explained by Tselios et al. [47], with the reaction of MAH groups of PP-g-MAH with the hydroxyl groups of GF. The generated carboxylic groups have the ability to form hydrogen bonds with the hydroxyl groups on GF.

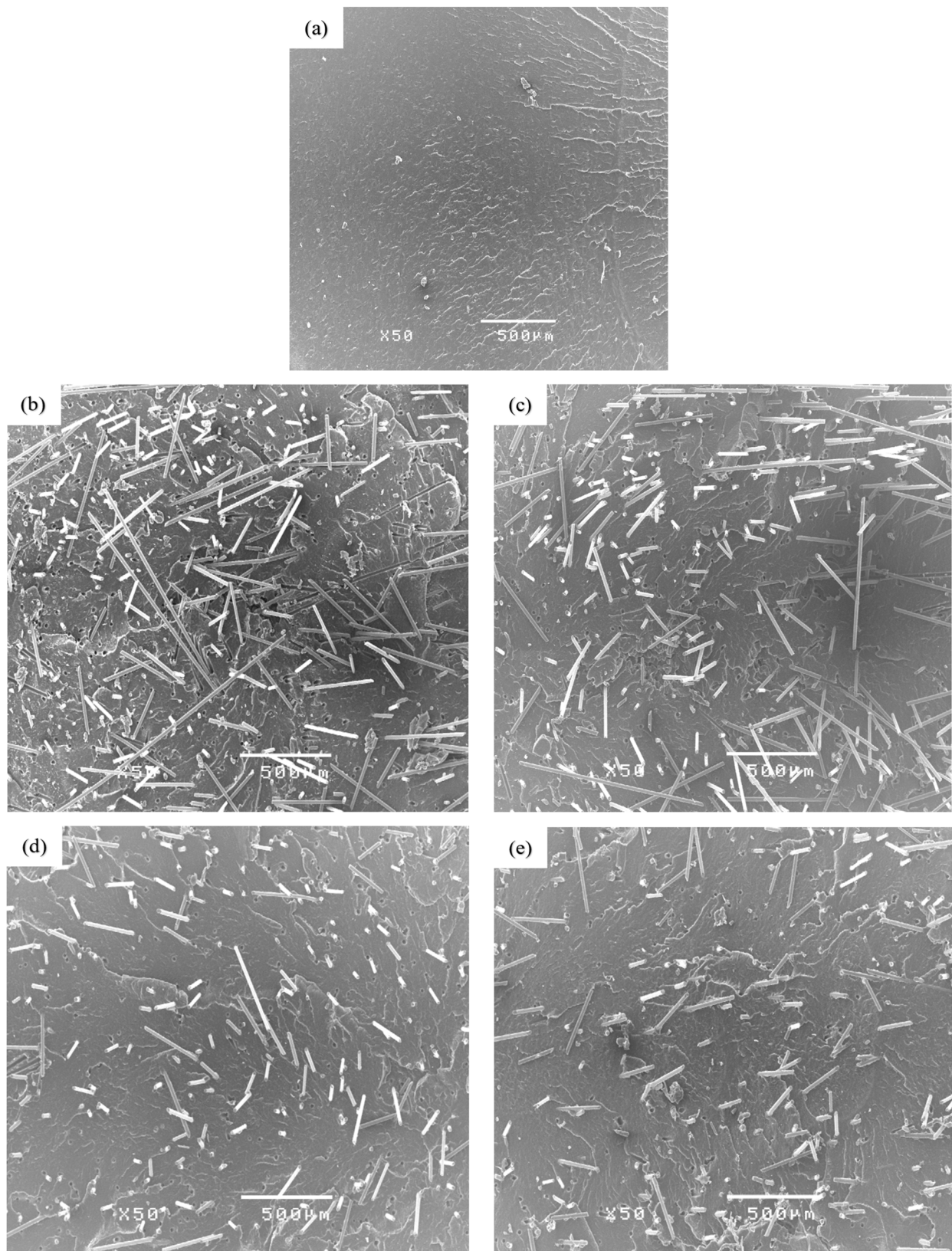


Figure 9. SEM micrographs at a magnification of 50× of (a) virgin PP, (b) LFTP devoid of PP-g-MAH, (c) LFTP with PP-g-MAH of 4 wt%, (d) LFTP with PP-g-MAH of 8 wt%, and (e) LFTP with PP-g-MAH of 12 wt%.

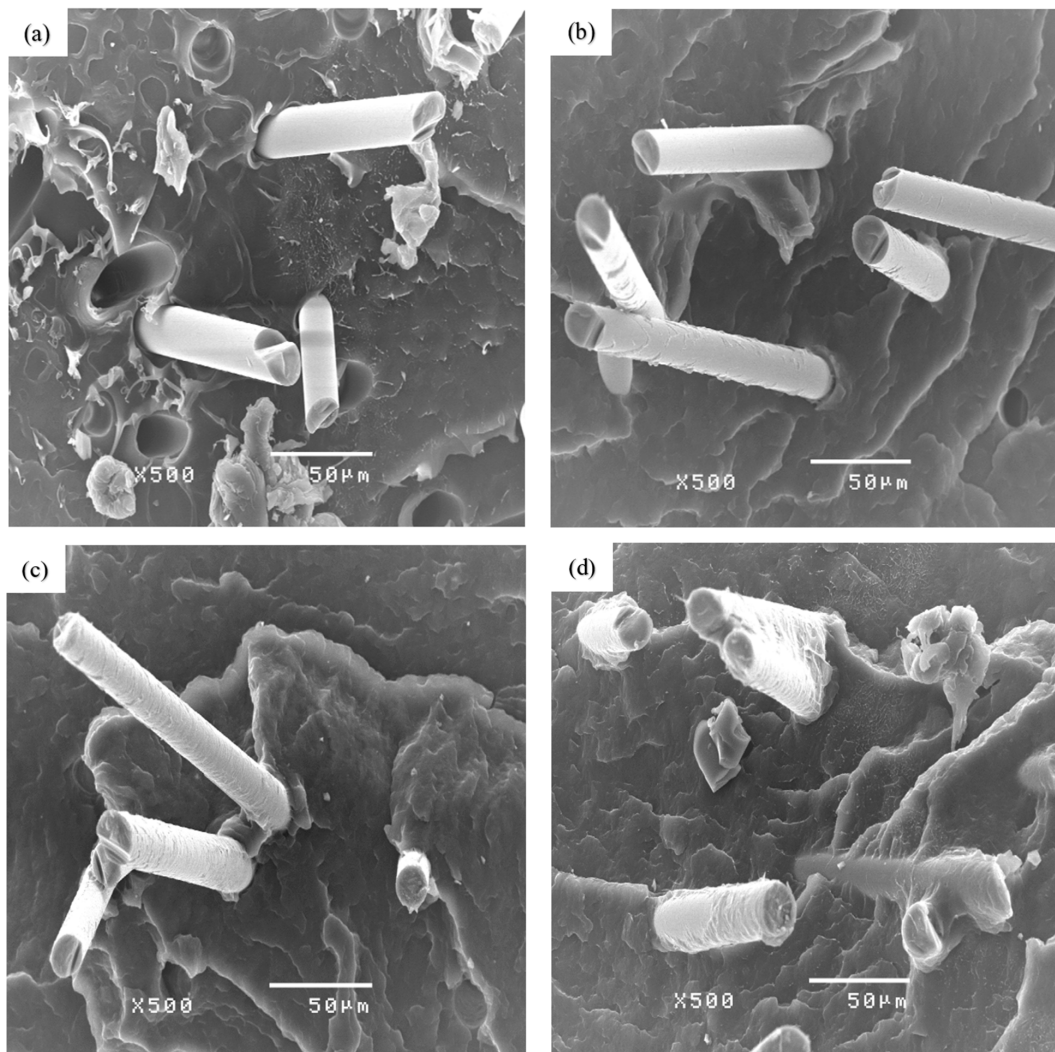


Figure 10. SEM micrographs at a magnification of $500\times$ of (a) LFTP devoid of PP-g-MAH, (b) LFTP with PP-g-MAH of 4 wt%, (c) LFTP with PP-g-MAH of 8 wt%, and (d) LFTP with PP-g-MAH of 12 wt%.

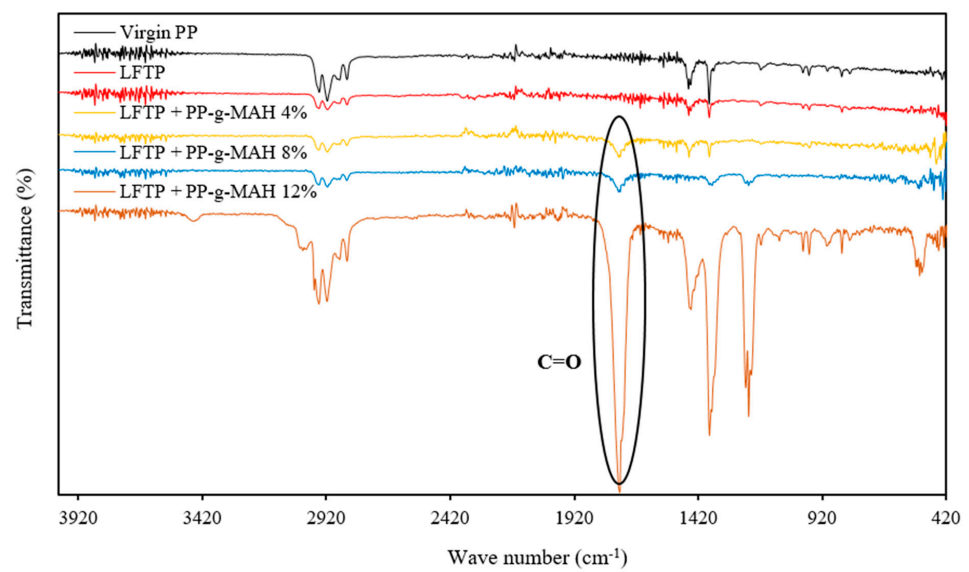


Figure 11. FTIR spectra of LFTPc with varying concentrations of PP-g-MAH.

3.5. A Comparison of Properties between LFTPc and Commercial LFT

The mechanical properties were conducted to compare with commercial LFTP at the same volume fraction of GF, which is 15 wt%, as depicted in Figure 12. The results clearly demonstrate that the mechanical properties of the LFTPc were better with the addition of PP-g-MAH. There was an approximate increase of 4.44–17.44% in the tensile modulus values, 42.25–59.26% in the tensile strength values, 9.07–20.72% in the flexural modulus values, 44.19–69.29% in the flexural strength values, and 18.16–50.33% in the impact property data. While the addition of PP-g-MAH into LFTP led to positive mechanical properties, exceeding the limit of PP-g-MAH addition will result in a reduction in impact strength, tensile modulus, and flexural modulus. Furthermore, the cost of PP-g-MAH incorporation into LFTPcs is taken into consideration. In comparison to the commercial LFTP product, the mechanical properties of the LFTPc devoid of PP-g-MAH have been found to be inferior. All mechanical property values in the LFTPc increased to levels that were comparable to commercial LFTP after PP-g-MAH was incorporated. The LFTPc containing filled PP-g-MAH component had a slightly greater tensile modulus, tensile strength, and flexural modulus values than commercial LFTP, by approximately 1–16.76%. The flexural strength values of the LFTPc incorporating PP-g-MAH content of 8 and 12 wt% were slightly higher than those of commercial LFTP, by approximately 7.17–10.87%. The impact strength values of the LFTPc containing a 4 wt% PP-g-MAH content were slightly greater compared to those of commercial LFTP by approximately 12.36%. Therefore, the LFTPc incorporated with a concentration of 4 wt% PP-g-MAH was considered optimal for manufacturing LFTP, as it exhibits nearly equivalent or higher mechanical properties compared to commercial LFTP. Although the flexural strength value was lower than those of commercial LFTP, it was only 5.57%.

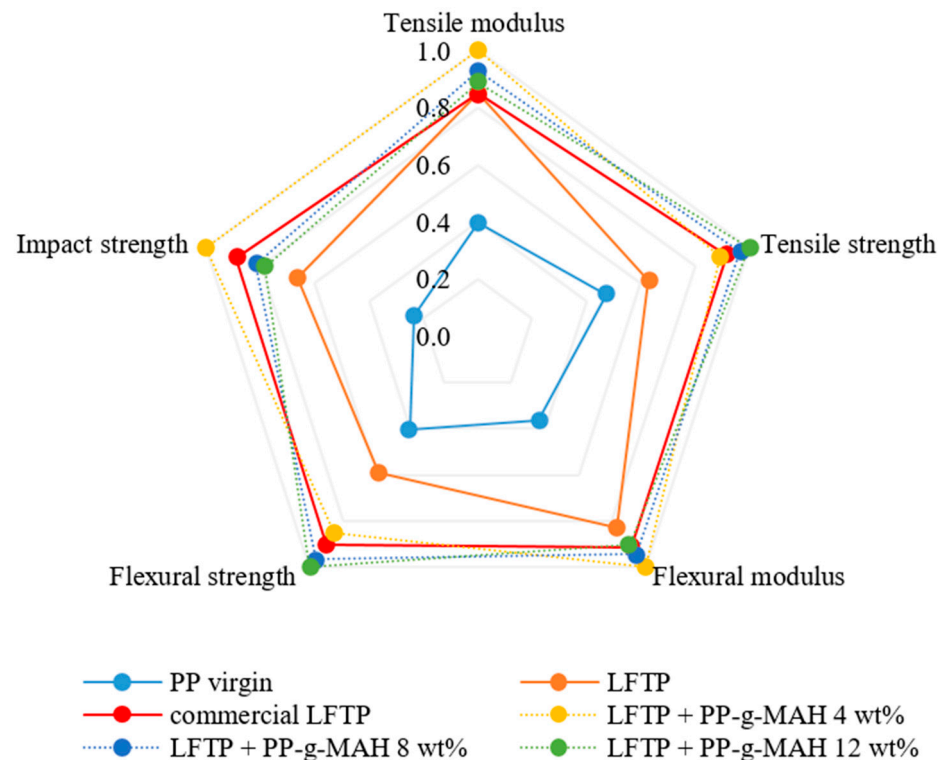


Figure 12. Comparison of properties between LFTPc and commercial LFT.

4. Conclusions

This study involved the incorporation of PP and GF into LFTP, a material produced using the thermoplastic pultrusion process. LFTP was incorporated with a varying PP-g-MAH content through injection molding for the preparation of specimens. The mechanical

properties of injection specimens were investigated, including tensile, flexural, and impact tests. The fiber length of LFTPc was measured to confirm the long fiber reinforcement. The morphology was examined to analyze the interfacial interaction between GF and PP, while FTIR was employed to study the differences in the chemical structure after incorporating PP-g-MAH into LFTPc. The study can be summarized as follows:

- Significant improvements were observed in the tensile modulus, flexural modulus, and impact strength of the LFTPc when an amount of 4 wt% PP-g-MAH was incorporated. Nevertheless, with the PP-g-MAH concentration exceeding 4 wt%, a decline in these properties was observed.
- The amount of PP-g-MAH added to LFTPc resulted in increases in both tensile and flexural strength. The enhanced interfacial bonding between GF and PP, along with the reduction in fiber pull-out, is the reason for this improvement. Therefore, the optimal concentration of PP-g-MAH for the LFTPc was found to be 4 wt%. This choice resulted in mechanical properties nearly equivalent to those of commercial products.
- The fiber length results indicate long fiber reinforcement, as there is a significant amount of fiber in the range of 3 to 6 mm of fiber length.

This research is significant because it contributes to the advancement of LFTP product development employing the thermoplastic pultrusion technique. It presents an alternative approach distinguished by affordable machinery costs and a straightforward process for LFTP production. In addition, the mechanical properties of LFTP from thermoplastic pultrusion are nearly equivalent to or higher than those of commercial LFTP. Thermoplastic pultrusion is an advanced process that should be further developed. In future research, thermoplastic pultrusion will be used for manufacturing hybrid long fiber pellets to enhance mechanical properties and improve product performance.

Author Contributions: Conceptualization, A.M. and P.T.; methodology, A.M. and P.T.; software, A.M. and P.T.; validation, A.M. and P.T.; formal analysis, A.M. and P.T.; investigation, A.M. and P.T.; resources, A.M. and P.T.; data curation, A.M. and P.T.; writing—original draft preparation, A.M. and P.T.; writing—review and editing, A.M. and P.T.; visualization, A.M. and P.T.; supervision, A.M. and P.T.; project administration, A.M. and P.T.; funding acquisition, A.M. and P.T.; All authors have read and agreed to the published version of the manuscript.

Funding: This research received no external funding.

Data Availability Statement: The data presented in this study are available on request from the corresponding author.

Acknowledgments: The Department of Industrial Engineering, Faculty of Engineering, Rajamangala University of Technology Thanyaburi, Thailand, has been acknowledged by the authors for allowing permission to utilize its laboratory equipment for the purpose of this research.

Conflicts of Interest: The authors declare no conflicts of interest. The funders had no role in the design of the study; in the collection, analyses, or interpretation of data; in the writing of the manuscript; or in the decision to publish the results.

References

1. Ning, H.; Lu, N.; Hassen, A.A.; Chawla, K.; Selim, M.; Pillay, S. A review of Long fibre-reinforced thermoplastic or long fibre thermoplastic (LFT) composites. *Int. Mater. Rev.* **2019**, *65*, 164–188. [[CrossRef](#)]
2. Duncan, R.K.; Chen, X.G.; Bult, J.B.; Brinson, L.C.; Schadler, L.S. Measurement of the critical aspect ratio and interfacial shear strength in MWNT/polymer composites. *Compos. Sci. Technol.* **2010**, *70*, 599–605. [[CrossRef](#)]
3. Migneault, S.; Koubaa, A.; Erchiqui, F.; Chaala, A.; Englund, K.; Wolcott, M.P. Application of micromechanical models to tensile properties of wood–plastic composites. *Wood Sci. Technol.* **2011**, *45*, 521–532. [[CrossRef](#)]
4. Kim, S.-E.; Ahn, J.-G.; Ahn, S.; Park, D.-H.; Choi, D.-H.; Lee, J.-C.; Yang, H.-I.; Kim, K.-Y. Development of PA6/GF Long-Fiber-Reinforced Thermoplastic Composites Using Pultrusion and Direct Extrusion Manufacturing Processes. *Appl. Sci.* **2022**, *12*, 4838. [[CrossRef](#)]
5. Alwekar, S.; Ogle, R.; Kim, S.; Vaidya, U. Manufacturing and characterization of continuous fiber-reinforced thermoplastic tape overmolded long fiber thermoplastic. *Compos. Part B Eng.* **2021**, *207*, 108597. [[CrossRef](#)]
6. Markarian, J. Long fibre reinforced thermoplastics continue growth in automotive. *Plast. Addit. Compd.* **2007**, *9*, 20–24. [[CrossRef](#)]

7. Balaji Thattai parthasarathy, K.; Pillay, S.; Ning, H.; Vaidya, U.K. Process simulation, design and manufacturing of a long fiber thermoplastic composite for mass transit application. *Compos. Part A Appl. Sci. Manuf.* **2008**, *39*, 1512–1521. [[CrossRef](#)]
8. Xie, T.; Yang, G. Interface and mechanical properties of poly(methyl methacrylate)-fiber composites. *J. Appl. Polym. Sci.* **2004**, *93*, 2478–2483. [[CrossRef](#)]
9. Krause, W.; Henning, F.; Tröster, S.; Geiger, O.; Eyerer, P. LFT-D—A Process Technology for Large Scale Production of Fiber Reinforced Thermoplastic Components. *J. Thermoplast. Compos. Mater.* **2003**, *16*, 289–302. [[CrossRef](#)]
10. Sheikh, M.R.; Hassan, A.; Yahya, R.; Mohd Isa, M.R.; Hussin, A.; Hornsby, P.R. Interfacial shear strength and tensile properties of injection-molded, short- and long-glass fiber-reinforced polyamide 6,6 composites. *J. Reinf. Plast. Compos.* **2011**, *30*, 1233–1242. [[CrossRef](#)]
11. Inoue, A.; Morita, K.; Tanaka, T.; Arao, Y.; Sawada, Y. Effect of screw design on fiber breakage and dispersion in injection-molded long glass-fiber-reinforced polypropylene. *J. Compos. Mater.* **2015**, *49*, 75–84. [[CrossRef](#)]
12. Kunc, V.; Frame, B.; Nguyen, B.; Tucker, C.; Velez-Garcia, G. Fiber length distribution measurement for long glass and carbon fiber reinforced injection molded thermoplastics. In Proceedings of the Automotive Composite Conference & Exhibition, Society of Plastics Engineers, Troy, MI, USA, 11–13 September 2007.
13. Van de Velde, K.; Kiekens, P. Thermoplastic pultrusion of natural fibre reinforced composites. *Compos. Struct.* **2001**, *54*, 355–360. [[CrossRef](#)]
14. Yang, C.; Wang, G.; Zhao, J.; Zhao, G.; Zhang, A. Lightweight and strong glass fiber reinforced polypropylene composite foams achieved by mold-opening microcellular injection molding. *J. Mater. Res. Technol.* **2021**, *14*, 2920–2931. [[CrossRef](#)]
15. Junaedi, H.; Baig, M.; Dawood, A.; Albahkali, E.; Almajid, A. Modeling analysis of the tensile strength of polypropylene base Short Carbon Fiber reinforced composites. *J. Mater. Res. Technol.* **2021**, *11*, 1611–1621. [[CrossRef](#)]
16. Rajak, D.K.; Wagh, P.H.; Linul, E. Manufacturing Technologies of Carbon/Glass Fiber-Reinforced Polymer Composites and Their Properties: A Review. *Polymers* **2021**, *13*, 3721. [[CrossRef](#)] [[PubMed](#)]
17. El-Ghaoui, K.; Chatelain, J.-F.; Ouellet-Plamondon, C. Effect of Graphene on Machinability of Glass Fiber Reinforced Polymer (GFRP). *J. Manuf. Mater. Process.* **2019**, *3*, 78. [[CrossRef](#)]
18. Tan, Y.; Wang, X.; Wu, D. Preparation, microstructures, and properties of long-glass-fiber-reinforced thermoplastic composites based on polycarbonate/poly(butylene terephthalate) alloys. *J. Reinf. Plast. Compos.* **2015**, *34*, 1804–1820. [[CrossRef](#)]
19. Hwang, D.; Cho, D. Fiber aspect ratio effect on mechanical and thermal properties of carbon fiber/ABS composites via extrusion and long fiber thermoplastic processes. *J. Ind. Eng. Chem.* **2019**, *80*, 335–344. [[CrossRef](#)]
20. Tipboonsri, P.; Memon, A. Optimizing thermoplastic pultrusion parameters for quality long fiber thermoplastic pellets in glass fiber-reinforced polypropylene. *Polym. Polym. Compos.* **2023**, *31*, 1–11. [[CrossRef](#)]
21. Tipboonsri, P.; Wattanahitsiri, V.; Memon, A. Long fiber thermoplastic pellets of glass fiber/polypropylene from pultrusion process. *J. Phys. Conf. Ser.* **2021**, *1719*, 012066. [[CrossRef](#)]
22. Minchenkov, K.; Vedernikov, A.; Safonov, A.; Akhatov, I. Thermoplastic Pultrusion: A Review. *Polymers* **2021**, *13*, 180. [[CrossRef](#)]
23. Tipboonsri, P.; Pramoonmak, S.; Uawongsuwan, P.; Memon, A. Optimization of Thermoplastic Pultrusion Parameters of Jute and Glass Fiber-Reinforced Polypropylene Composite. *Polymers* **2024**, *16*, 83. [[CrossRef](#)]
24. Memon, A.; Nakai, A. Mechanical Properties of Jute Spun Yarn/PLA Tubular Braided Composite by Pultrusion Molding. *Energy Procedia* **2013**, *34*, 818–829. [[CrossRef](#)]
25. Nordin, N.A.; Yussof, F.M.; Kasolang, S.; Salleh, Z.; Ahmad, M.A. Wear Rate of Natural Fibre: Long Kenaf Composite. *Procedia Eng.* **2013**, *68*, 145–151. [[CrossRef](#)]
26. Yadav, R.; Tirumali, M.; Wang, X.; Naebe, M.; Kandasubramanian, B. Polymer composite for antistatic application in aerospace. *Def. Technol.* **2020**, *16*, 107–118. [[CrossRef](#)]
27. Lin, J.-H.; Huang, C.-L.; Liu, C.-F.; Chen, C.-K.; Lin, Z.-I.; Lou, C.-W. Polypropylene/Short Glass Fibers Composites: Effects of Coupling Agents on Mechanical Properties, Thermal Behaviors, and Morphology. *Materials* **2015**, *8*, 8279–8291. [[CrossRef](#)]
28. Wenzhong, N. The effect of coupling agents on the mechanical properties of carbon fiber-reinforced polyimide composites. *J. Thermoplast. Compos. Mater.* **2015**, *28*, 1572–1582. [[CrossRef](#)]
29. Denault, J.; Vu-Khanh, T. Fiber/Matrix Interaction in Carbon/PEEK Composites. *J. Thermoplast. Compos. Mater.* **1993**, *6*, 190–204. [[CrossRef](#)]
30. Chen, M.; Wan, C.; Zhang, Y.; Zhang, Y. Fibre Orientation and Mechanical Properties of Short Glass Fibre Reinforced PP Composites. *Polym. Polym. Compos.* **2005**, *13*, 253–262. [[CrossRef](#)]
31. Nayak, S.K.; Mohanty, S. Sisal Glass Fiber Reinforced PP Hybrid Composites: Effect of MAPP on the Dynamic Mechanical and Thermal Properties. *J. Reinf. Plast. Compos.* **2010**, *29*, 1551–1568. [[CrossRef](#)]
32. Abd Rahman, N.M.M.; Hassan, A.; Yahya, R. Extrusion and injection-molding of glass fiber/MAPP/polypropylene: Effect of coupling agent on DSC, DMA, and mechanical properties. *J. Reinf. Plast. Compos.* **2011**, *30*, 215–224. [[CrossRef](#)]
33. Kim, H.-S.; Lee, B.-H.; Choi, S.-W.; Kim, S.; Kim, H.-J. The effect of types of maleic anhydride-grafted polypropylene (MAPP) on the interfacial adhesion properties of bio-flour-filled polypropylene composites. *Compos. Part A Appl. Sci. Manuf.* **2007**, *38*, 1473–1482. [[CrossRef](#)]
34. Gümüş, B. Effect of MA-g-PP addition on mechanical properties of polypropylene/hollow glass spheres/nanoclay composites. *Polym. Bull.* **2022**, *80*, 3405–3422. [[CrossRef](#)]

35. Kim, Y.; Park, O.O. Effect of Fiber Length on Mechanical Properties of Injection Molded Long-Fiber-Reinforced Thermoplastics. *Macromol. Res.* **2020**, *28*, 433–444. [[CrossRef](#)]
36. Fu, X.; He, B.; Chen, X. Effects of Compatibilizers on Mechanical Properties of Long Glass Fiber-Reinforced Polypropylene. *J. Reinf. Plast. Compos.* **2009**, *29*, 936–949. [[CrossRef](#)]
37. ASTM D638-14; Standard Test Method for Tensile Properties of Plastics. ASTM International: West Conshohocken, PA, USA, 2020.
38. ASTM D790-10; Standard Test Method for Flexural Properties of Unreinforced and Reinforced Plastics and Electrical Insulating Materials. ASTM International: West Conshohocken, PA, USA, 2016.
39. ASTM D256-10; Standard Test Methods for Determining the Izod Pendulum Impact Resistance of Plastics. ASTM International: West Conshohocken, PA, USA, 2015.
40. Wong, K.H.; Syed Mohammed, D.; Pickering, S.J.; Brooks, R. Effect of coupling agents on reinforcing potential of recycled carbon fibre for polypropylene composite. *Compos. Sci. Technol.* **2012**, *72*, 835–844. [[CrossRef](#)]
41. Tharanikkarasu, K.; Kim, B. Modification of aqueous polyurethane dispersions via tetraphenylethane iniferters. *J. Appl. Polym. Sci.* **1999**, *73*, 2993–3000. [[CrossRef](#)]
42. Abbasian, M.; Ghaemini, H.; Jaymand, M. A facile and efficient strategy for the functionalization of multiple-walled carbon nanotubes using well-defined polypropylene-grafted polystyrene. *Appl. Phys. A* **2018**, *124*, 522. [[CrossRef](#)]
43. Lian, Z.; Xu, Y.; Zuo, J.; Qian, H.; Luo, Z.; Wei, W. Preparation of PP-g-(AA-MAH) Fibers Using Suspension Grafting and Melt-Blown Spinning and its Adsorption for Aniline. *Polymers* **2020**, *12*, 2157. [[CrossRef](#)]
44. Burgada, F.; Fages, E.; Quiles-Carrillo, L.; Lascano, D.; Ivorra-Martinez, J.; Arrieta, M.P.; Fenollar, O. Upgrading Recycled Polypropylene from Textile Wastes in Wood Plastic Composites with Short Hemp Fiber. *Polymers* **2021**, *13*, 1248. [[CrossRef](#)]
45. Fan, M.; Zhang, Y.; Li, X.; Zeng, B.; Chen, S.; Zhu, W.; Wang, S.; Xu, J.; Feng, N. Facile synthesis and applications of polypropylene/polydimethylsiloxane graft copolymer. *Polym. Adv. Technol.* **2019**, *30*, 1226–1233. [[CrossRef](#)]
46. Martinez, G.; Sanchez, S.; Ramos, L.; Perez, O.; Ramirez, E.; Benavides-Cantú, R.; Avila-Orta, C.; Cruz, V.; Mata, J.; Lozano-Ramirez, T.; et al. Aniline-Modified Polypropylene as a Compatibilizer in Polypropylene Carbon Nanotube Composites. *Polym.-Plast. Technol. Eng.* **2017**, *57*, 1360–1366. [[CrossRef](#)]
47. Tselios, C.; Bikiaris, D.; Savidis, P.; Panayiotou, C.; Larena, A. Glass-fiber reinforcement of in situ compatibilized polypropylene/polyethylene blends. *J. Mater. Sci.* **1999**, *34*, 385–394. [[CrossRef](#)]

Disclaimer/Publisher’s Note: The statements, opinions and data contained in all publications are solely those of the individual author(s) and contributor(s) and not of MDPI and/or the editor(s). MDPI and/or the editor(s) disclaim responsibility for any injury to people or property resulting from any ideas, methods, instructions or products referred to in the content.